ISSN 0021-3640, JETP Letters, 2016, Vol. 103, No. 6, pp. 390–394. © Pleiades Publishing, Inc., 2016.

CONDENSED MATTER

Pade Spectroscopy of Structural Correlation Functions: Application to Liquid Gallium[1]

N. M. Chtchelkatchev[a, b], B. A. Klumov[a, c, d], R. E. Ryltsev[a, e, f], R. M. Khusnutdinoff[a, g], and A. V. Mokshin[a, g]

[a] *Landau Institute for Theoretical Physics, Russian Academy of Sciences, Chernogolovka, Moscow region, 142432 Russia*

[b] *Moscow Institute of Physics and Technology (State University), Institutskii per. 9, Dolgoprudnyi, Moscow region, 141700 Russia*

[c] *Joint Institute for High Temperatures, Russian Academy of Sciences, Moscow, 125412 Russia*

[d] *Aix-Marseille-Université, CNRS, Laboratoire PIIM, UMR 7345, 13397 Marseille, France*

[e] *Institute of Metallurgy, Ural Branch, Russian Academy of Sciences, Yekaterinburg, 620016 Russia*

[f] *Ural Federal University, Yekaterinburg, 620002 Russia*

[g] *Kazan (Volga Region) Federal University, Kazan, 420008 Russia*

e-mail: nms@itp.ac.ru

Received February 2, 2016; in final form, February 18, 2016

We propose the new method of fluid structure investigation based on numerical analytic continuation of structural correlation functions with Pade approximants. The method particularly allows extracting hidden structural features of disordered condensed matter systems from experimental diffraction data. The method has been applied to investigate the local order of liquid gallium, which has a non-trivial structure in both the liquid and solid states. Processing the correlation functions obtained from molecular dynamic simulations, we show the method proposed reveals non-trivial structural features of liquid gallium such as the spectrum of length-scales and the existence of different types of local clusters in the liquid.

DOI: 10.1134/S0021364016060035

INTRODUCTION

Gallium is a very specific metal [1]. First of all, it has enormously large domain of its phase diagram corresponding to liquid state. For example, the temperature interval of stable liquid state at ambient pressure is (302.93, 2477) K. Diffraction experiments have shown that the local structure of liquid gallium is very complicated and it differs much from the local structure of typical simple liquids [2–5]. Accordingly, the crystal structure of gallium is also nontrivial: below its melting temperature $T_m = 302.93$ K at the ambient pressure the stable phase corresponds to the orthorhombic lattice, which is atypical for single-component metallic systems [6] (amount the other metals, the only Eu has the same lattice structure at ambient pressure). At higher pressures, there are many polymorphic transitions to other nontrivial crystal structures [7, 8].

Last time, a lot of theoretical efforts were concentrated on investigation of the local structures and anomalies of gallium in liquid phase [9–12]. However, there is a gap between theoretical investigations of gallium and experiment. The main problem is that the only way to directly access the local structure is molecular dynamics (MD) simulations, which cannot unambiguously describe structure of real materials. Indeed, classical MD deals with model approximate potentials and first-principles MD has a problem of restricted spatial and time scales available in simulations. Experiment also cannot directly access the local structure: the information about angle correlations is mostly lost in the static structure factor or radial distribution function (RDF); so only radial correlations can be extracted. Here, we develop a new method of correlation function processing based on complex analysis with Pade approximants.

Using this method, we study local structure of liquid gallium and extract its non-trivial features. Analyzing structural correlation functions obtained from MD simulations with EAM potentials, we extract the spectrum of spatial length scales and the existence of two types of local clusters. We show that the best fit of the gallium RDF can be performed using Lorentzians instead of Gaussians, which are usually used for that purpose.

[1] The article is published in the original. See the supplemental material for this paper at www.jetpletters.ac.ru.

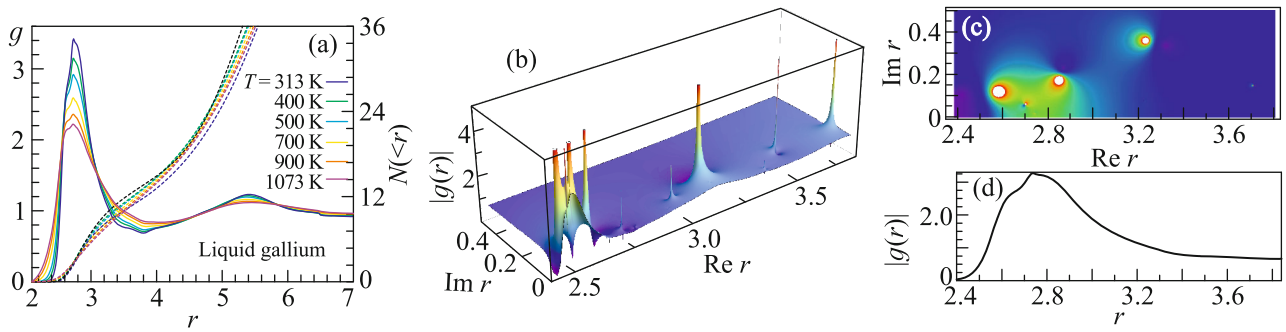

Fig. 1. (Color online) Pade spectroscopy of the radial distribution function. (a) (Solid lines) Radial distribution function $g(r)$ of liquid gallium and (dashed lines) its distance-dependent coordination number $N(< r)$ at different temperatures T (indicated on the plot). (b)–(d) Liquid gallium, $T = 500$ K. (b) Doing the Pade approximation, we find characteristic scales of gallium for particle distribution in the first coordination sphere: $r = 2.58$, 2.69, 2.84 Å. The scale $r = 3.33$ Å corresponds to the tail of the first coordination sphere. (c) Density plot of the Pade approximant. (d) First peak of $g(r)$.

LOCAL ORDER OF GALLIUM

For MD simulations of liquid gallium, we have used LAMMPS molecular dynamics package. The system of $N = 20000$–100000 particles interacting via EAM potential [13], specially designed for gallium [14], was simulated under periodic boundary conditions in Nose–Hoover NPT ensemble. This amount of particles is enough to obtain satisfactory results. More simulation details can be found in [15] where a similar simulation was described. We checked that radial distribution functions obtained by our simulation quantitatively agree with those extracted from experiment [15].

Here, we focus on gallium at ambient pressure and investigate how its properties in liquid state depend on temperature. Figure 1a shows the radial distribution function $g(r)$ of gallium taken for several temperatures in the range of (313, 1073) K. The distance-dependent coordination number $N(< r) \equiv 4\pi\rho\int_0^r r'^2 g(r')dr'$, which is the mean number of particles inside a sphere of radius r, is also plotted in Fig. 1a; in part, the distance-dependent coordination number $N(< r)$ shows the number of nearest neighbors in the first coordination shell.

It is clear from the figure that the shape of the first RDF peak is nontrivial. It can be seen that the first RDF peak of gallium has a clear shoulder. Particles forming the local clusters are mostly located at distances corresponding to the first coordination sphere (first peak of RDF). That suggests that local structure of liquid gallium is rather nontrivial. More detailed information can be extracted only after specific processing of RDF.

The promising way to extract features of local order hidden in RDF is performing analytic continuation to complex plane of distances. This is usual way in the theory of correlation functions of quantum systems especially for analytic continuation of the Greens functions from imaginary (Matsubara [16]) frequencies to the real frequency domain [17–19]. Recently, the method of numerical analytic continuation was successfully applied to investigations of velocity autocorrelation function of Lennard-Jones (LJ) fluid [20, 21] and in classical hydrodynamics of the Stokes waves [22]. Here we use this method for analysis of gallium RDFs. For numerical analytic continuation we build the Pade approximant [23, 24] as was done in [17, 21]. More details can be found in the supplemental material for this paper in [25].

The static structure factor is related to RDF as [26]:

$$S(k) = 1 + \frac{4\pi}{\rho}\mathrm{Im}\int_0^\infty r[g(r) - 1]e^{ikr}dr. \quad (1)$$

Therefore, if $g(r)$ has a pole, at the position r_p, we should expect that the contribution of this pole to the structure factor oscillates as $\cos(k\mathrm{Re}r_p)$ or $\sin(k\mathrm{Re}r_p)$ and decays with k as $e^{-k\,\mathrm{Im}\,r_p}$. Thus, knowledge of the poles gives important scales characterizing the particle system.

In Figs. 1b and 1c, we show the results of the typical processing of gallium RDF by Pade approximants. As follows, we use the Pade approximant of RDF for its analytic continuation in complex-r. Figure 1b shows the absolute value of RDF in complex-r plane while the peaks correspond to the poles. We see a limited number of poles near the real axis: so the Lorenzian fit of RDF perfectly matches all its basic features, see Figs. 1c and 1d. The real parts of the positions of the poles are important length scales characterizing gallium: as follows, in the first coordination sphere: $r = 2.58$, 2.69, 2.84 Å; the scale $r = 3.33$ Å corresponds to the tail of the first coordination sphere. These scales are in fact characteristic interparticle distances in the first coordination shell. Thus, we see that analytic continuation with Pade approximants allows extracting multi-scale character of local structure of liquid gallium. In that connection, remember that, at ambient pressure, gallium crystallizes into non-trivial ort-

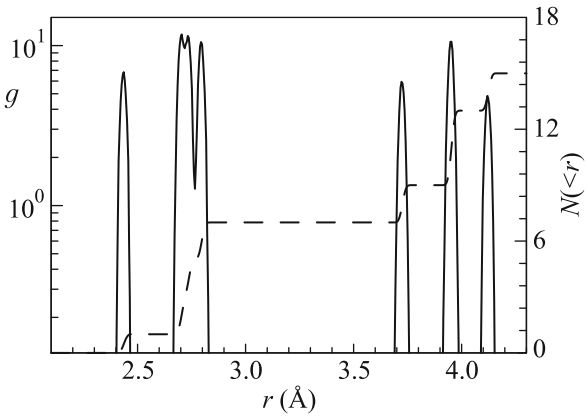

Fig. 2. Radial distribution function obtained for the ideal lattice of α-Ga with small random noise, which mimics thermal vibrations. The distance-dependent coordination number $N(< r)$ is also plotted by the dashed line to evaluate the number of atoms at different shells.

horhombic lattice and so it is interesting to find relation between unusual multiscale local order of the liquid and non-trivial crystal symmetry.

In Fig. 2, we show RDF obtained for ideal lattice of α-Ga (orthorhombic) with small random noise which mimics thermal vibrations. We see that first coordination shell contains two atoms located at short distance of 2.46 Å. Such Ga_2 dimers were earlier suggested to be formed by covalent-like bonding [27]. Each Ga atom has other six nearest neighbors located in pairs in different coordination shells at distances 2.7, 2.73, 2.79 Å. Therefore, the crystal structure of α-Ga demonstrates spectrum of spatial scales. The comparison of these scales with those obtained from analytic continuation of RDF shows good agreement. Indeed the ratios of maximal and minimal distances are 1.134 for experimental lattice structure and 1.1 for scales extracted from liquid RDF. Of course, the analytic continuation of liquid RDF does not distinct two nearly located scales. Recently, the similar analysis of liquid Ga structure was performed in [15] where simulated RDF were approximated by a set of Gaussians that gave similar interval of spatial scales. However, this method can distinct only two scales in mentioned interval. Moreover, the results strongly depend on the choice of approximation parameters such as the number and the shape of approximating functions [25].

For comparison we investigated LJ fluid and saw, unlike Gallium, two merging poles deep in the complex plain corresponding to the first peak of RDF. The poles show one characteristic scale—maximum of RDF [25].

ORIENTATIONAL ORDER OF GALLIUM

More detailed structural information can be obtained from analysis of the local orientational order. The simplest way to describe it is calculating angular distribution function $P(\theta)$ which is probability density of angle θ between two vectors connecting a particle with its two nearest neighbors.

Figure 3 shows bond angle distribution functions of liquid gallium at different temperatures T (indicated on the plot). Additionally the BADF of LJ-melt (which is nearly universal on the LJ melting curve) is also plotted for the comparison. Figures 3b–3d show BADF for T = 500 K. Looking at BADFs at real-θ axis, it is difficult to say something specific about the clusters forming the local order. However, after its processing with the Pade approximant, we see a number of poles in complex-θ plane. The positions of poles (Re θ) give characteristic angles between the particles forming the local order clusters. In particular, we see two pronounced poles at the vicinity of the first peak, which are located near the angles 45 and 60. The value

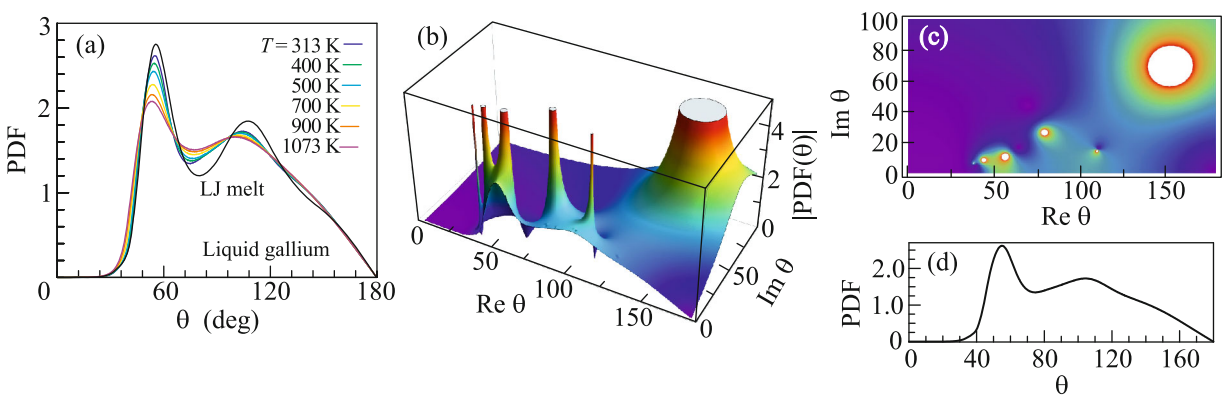

Fig. 3. (Color online) Pade spectroscopy of the bond angle distribution function (BADF). (a) Bond angle distribution function of liquid gallium at different temperatures T (indicated on the plot). The bond angle distribution function of the LJ melt (which is nearly universal on the LJ melting curve) is also plotted for comparison. (b–d) Bond angle distribution function for T = 500 K and its processing with Pade approximant. We see a number of poles; their positions (Re θ) give characteristic angles between the particles forming local order clusters.

of $\theta = 60$ is typical for simple liquids and corresponds to tetrahedral local order [28]. However, the angle $\theta = 45$ suggests non-trivial symmetry of local clusters probably caused by the existence of short-bonded particles revealed by RDF analysis.

Another way to analyze the orientational order is the well-known bond order parameter method, which is widely used to characterize order in simple fluids, solids and glasses [29–33], hard spheres [34, 35], colloidal suspensions [36], complex plasmas [37–39], and metallic glasses [40].

Each particle i is connected via vectors (bonds) with its $N_{nn}(i)$ nearest neighbors (NN), and the rotational invariants (RIs) of rank l of second $q_l(i)$ and third $w_l(i)$ orders are calculated as:

$$q_l(i) = \left[\frac{4\pi}{2l+1}\sum_{m=-l}^{l}|q_{lm}(i)|^2\right]^{1/2}, \quad (2)$$

$$w_l(i) = \sum_{\substack{m_1,m_2,m_3\\ m_1+m_2+m_3=0}} \begin{bmatrix} l & l & l\\ m_1 & m_2 & m_3\end{bmatrix} q_{lm_1}(i)q_{lm_2}(i)q_{lm_3}(i), \quad (3)$$

where $q_{lm}(i) = N_{nn}(i)^{-1}\sum_{j=1}^{N_{nn}(i)} Y_{lm}(\mathbf{r}_{ij})$, Y_{lm} are the spherical harmonics and $\mathbf{r}_{ij} = \mathbf{r}_i - \mathbf{r}_j$ are the vectors connecting the centers of particles i and j. In Eq. (3), $\begin{bmatrix} l & l & l\\ m_1 & m_2 & m_3\end{bmatrix}$ are the Wigner 3j-symbols, and the summations performed over all the indexes $m_i = -l, \ldots, l$ satisfying the condition $m_1 + m_2 + m_3 = 0$. As was shown in the pioneering work [29], the bond order parameters q_l and w_l can be used as measures to characterize the local orientational order and the phase state of considered systems.

Table

Lattice type	q_4	q_6	w_4	w_6
hcp (12 NN)	0.097	0.485	0.134	–0.012
fcc (12 NN)	0.19	0.575	–0.159	–0.013
ico (12 NN)	1.4×10^{-4}	0.663	–0.159	–0.169
bcc (8 NN)	0.5	0.628	–0.159	0.013
bcc (14 NN)	0.036	0.51	0.159	0.013
LJ melt (12 NN)	≈0.155	≈0.37	≈–0.023	≈–0.04

Because each lattice type has a unique set of bond order parameters, the method of RIs can also be used to identify lattice and liquid structures in mixed systems. The values of q_l and w_l for a few common lattice types (including liquid-like Lennard-Jones melt) are presented in table.

To quantify the local orientational order, it is also convenient to use the probability distribution functions (PDFs) $P(q_l)$ and $P(w_l)$. Figure 4 shows the PDFs at different l ($l = 4, 6$) at different temperatures of liquid gallium in comparison to those calculated for LJ liquid [25, 28] whose PDFs are nearly universal along the melting line. We see again that such PDFs calculated at real-q_l axis (Figs. 4a and 4b) reveal no interesting features of liquid gallium structure. We see broad dome-shaped distributions, which are similar to those for LJ liquids [25]. But analytic continuation in the complex-q plane reveals that $P(q_l)$ are in fact composed of two Lorenzian-like peaks with similar values of both the maximum location (Re(q)) and peak width (Im(q)).

This fact suggests the structure of liquid gallium consists of two types of local order that is in agreement with the earlier obtained results [5, 11].

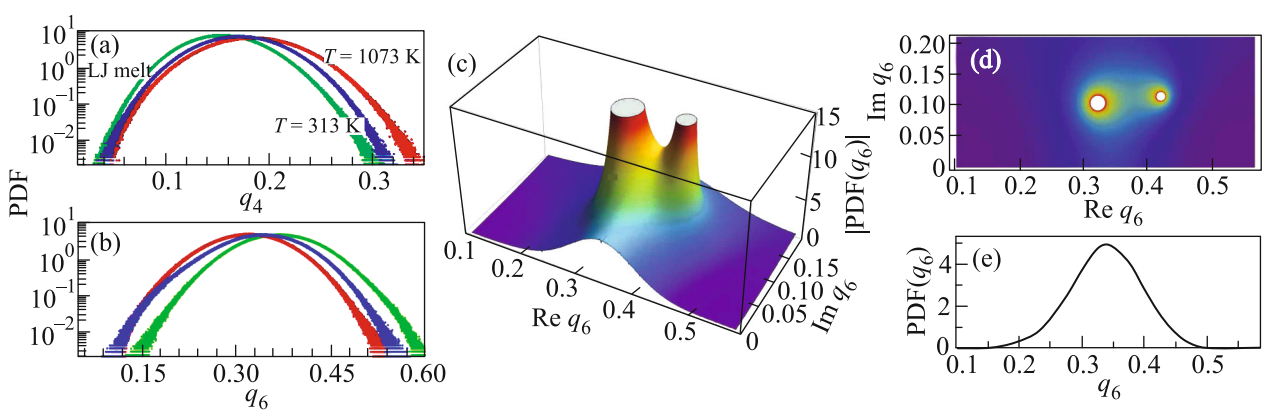

Fig. 4. (Color online) Pade spectroscopy of probability distribution functions (PDFs). (a, b) Orientational local order of liquid gallium: PDFs of the bond order parameters q_l ($l = 4, 6$) at two temperatures $T =$ (blue line) 313 and (red line) 1073 K. Green solid lines represent the same PDFs for the LJ melt taken on the melting line (it can be shown that along the melting line these PDFs are practically universal). (c, d) Absolute value of PDF ($l = 6$) of gallium for $T = 500$ K in complex q_6-plane. (e) Probability distribution function of gallium for $T = 500$ K plotted for comparison with poles of the Pade approximant in panel d. The poles are situated at Re $q_6 = 0.32, 0.42$.

CONCLUSIONS

We have proposed the new method of fluid structure investigation based on numerical analytic continuation of structural data obtained from both experiment and computer simulations. The method particularly allows extracting hidden structural features of disordered condensed matter systems from experimental diffraction data. The method has been applied to investigate the local order of liquid gallium, which is supposed to have complex structure. We show that analytic continuation of structural correlation functions such as radial distribution function, bond angle distribution function and bond orientational order parameters reveals non-trivial structural features of liquid. Firstly, we show that, processing the liquid RDF, our method allows easily obtaining the spectrum of length-scales, which are in close agreement with those for crystal state. Secondly, we show for the first time that correlation functions of orientational order also have non-trivial features probably caused by the existence of different types of local clusters in the liquid.

We are grateful to V. Brazhkin and D. Belashchenko for stimulating discussions. This work was supported by the Russian Science Foundation (project no. 14-12-01185). The work of B.A.K. was supported by the "Investissements d'Avenir" French Government program (A*MIDEX grant no. ANR-11-IDEX-0001-02). We are grateful to the Russian Academy of Sciences and the National Research Centre Kurchatov Institute for access to JSCC and HPC supercomputers. Access to the Uran cluster from the Institute of Metallurgy, Ural Branch, Russian Academy of Sciences was supported by the Government of the Russian Federation (Act 211, contract no. 02.A03.21.0006).

REFERENCES

1. Y. Waseda, *The Structure of Non-Crystalline Materials: Liquids and Amorphous Solids* (McGraw-Hill, New York, 1980).
2. A. H. Narten, J. Chem. Phys. **56**, 5681 (1972).
3. Y. Waseda and K. Suzuki, Phys. Status Solidi B **49**, 339 (1972).
4. A. Lyapin, E. Gromnitskaya, O. Yagafarov, O. Stalgorova, and V. Brazhkin, J. Exp. Theor. Phys. **107**, 818 (2008).
5. O. F. Yagafarov, Y. Katayama, V. V. Brazhkin, A. G. Lyapin, and H. Saitoh, Phys. Rev. B **86**, 174103 (2012).
6. A. F. Wells, *Structural Inorganic Chemistry* (Oxford Univ. Press, Oxford, 2012).
7. O. Schulte and W. B. Holzapfel, Phys. Rev. B **55**, 8122 (1997).
8. T. Kenichi, K. Kazuaki, and A. Masao, Phys. Rev. B **58**, 2482 (1998).
9. S.-F. Tsay and S. Wang, Phys. Rev. B **50**, 108 (1994).
10. X. G. Gong, G. L. Chiarotti, M. Parrinello, and E. Tosatti, Europhys. Lett. **21**, 469 (1993).
11. J. Yang, J. S. Tse, and T. Iitaka, J. Chem. Phys. **135**, 044507 (2011).
12. K. H. Tsai, T.-M. Wu, and S.-F. Tsay, J. Chem. Phys. **132**, 034502 (2010).
13. D. K. Belashchenko, Phys. Usp. **56**, 1176 (2013).
14. D. Belashchenko, Russ. J. Phys. Chem. A **86**, 779 (2012).
15. A. Mokshin, R. Khusnutdinoff, A. Novikov, N. Blagoveshensky, and A. Puchkov, J. Exp. Theor. Phys. **121**, 828 (2015).
16. A. A. Abrikosov, L. P. Gorkov, and I. E. Dzyaloshinski, *Methods of Quantum Field Theory in Statistical Physics* (Dover, New York, 1975).
17. H. Vidberg and J. Serene, J. Low Temp. Phys. **29**, 179 (1977).
18. H. Yamada and K. Ikeda, Eur. Phys. J. B **87**, 1 (2014).
19. J. Schött, I. L. Locht, E. Lundin, O. Grånäs, O. Eriksson, and I. Marco, arXiv:1511.03496 (2015).
20. S. H. Krishnan and K. G. Ayappa, J. Chem. Phys. **118**, 690 (2003).
21. N. Chtchelkatchev and R. Ryltsev, Pis'ma Zh. Eksp. Teor. Fiz. **102**, 732 (2015).
22. S. Dyachenko, P. Lushnikov, and A. Korotkevich, JETP Lett. **98**, 675 (2014).
23. G. A. Baker and P. R. Graves-Morris, *Padé Approximants*, Vol. 59 of *Encyclopedia of Mathematics and Its Applications* (Cambridge Univ. Press, Cambridge, 1996).
24. http://mathworld.wolfram.com/PadeApproximant.html
25. www.jetpletters.ac.ru.
26. J.-P. Hansen and I. R. McDonald, *Theory of Simple Liquids: With Applications to Soft Matter* (Academic, Amsterdam, 2013).
27. X. G. Gong, G. L. Chiarotti, M. Parrinello, and E. Tosatti, Phys. Rev. B **43**, 14277 (1991).
28. R. E. Ryltsev and N. M. Chtchelkatchev, Phys. Rev. E **88**, 052101 (2013).
29. P. J. Steinhardt, D. R. Nelson, and M. Ronchetti, Phys. Rev. B **28**, 784 (1983).
30. P. J. Steinhardt, D. R. Nelson, and M. Ronchetti, Phys. Rev. Lett. **47**, 1297 (1981).
31. J. R. Errington, J. Chem. Phys. **118**, 2256 (2003).
32. P. R. ten Wolde, M. J. Ruiz-Montero, and D. Frenkel, J. Chem. Phys. **104**, 9932 (1996).
33. B. Klumov, JETP Lett. **97**, 327 (2013).
34. M. D. Rintoul and S. Torquato, J. Chem. Phys. **105**, 9258 (1996).
35. B. A. Klumov, S. A. Khrapak, and G. E. Morfill, Phys. Rev. B **83**, 184105 (2011).
36. U. Gasser, E. R. Weeks, A. Schofield, P. N. Pusey, and D. A. Weitz, Science **292**, 258 (2001).
37. M. Rubin-Zuzic, G. E. Morfill, A. V. Ivlev, R. Pompl, B. A. Klumov, W. Bunk, H. M. Thomas, H. Rothermel, O. Havnes, and A. Fouquát, Nature Phys. **2**, 181 (2006).
38. B. A. Klumov, Phys. Usp. **53**, 1053 (2010).
39. S. A. Khrapak, B. A. Klumov, P. Huber, V. I. Molotkov, A. M. Lipaev, V. N. Naumkin, H. M. Thomas, A. V. Ivlev, G. E. Morfill, O. F. Petrov, V. E. Fortov, Y. Malentschenko, and S. Volkov, Phys. Rev. Lett. **106**, 205001 (2011).
40. A. Hirata, L. J. Kang, T. Fujita, B. Klumov, K. Matsue, M. Kotani, A. R. Yavari, and M. W. Chen, Science **341**, 376 (2013).